



Technical Note

# Eutrophication and HAB Occurrence Control in Lakes of Different Origins: A Multi-Source Remote Sensing Detection Strategy

Giovanni Laneve <sup>1</sup>, Alejandro Téllez <sup>1</sup>, Ashish Kallikkattil Kuruvila <sup>1</sup>, Milena Bruno <sup>2</sup>  
and Valentina Messineo <sup>2,\*</sup>

<sup>1</sup> Earth Observation Satellite Images Applications Lab, “La Sapienza” University, Via Salaria 851, 00138 Rome, Italy; giovanni.laneve@uniroma1.it (G.L.); do\_carvajal@hotmail.com (A.T.); kallikkattilkuruvila.1918117@studenti.uniroma1.it (A.K.K.)

<sup>2</sup> Technical-Scientific Service Core Facilities, Istituto Superiore di Sanità, Viale Regina Elena 299, 00161 Rome, Italy; milena.bruno@iss.it

\* Correspondence: valentina.messineo@iss.it

**Abstract:** Remote sensing techniques have become pivotal in monitoring algal blooms and population dynamics in freshwater bodies, particularly to assess the ecological risks associated with eutrophication. This study focuses on remote sensing methods for the analysis of 4 Italian lakes with diverse geological origins, leveraging water quality samples and data from the Sentinel-2 and Landsat 5.7–8 platforms. Chl-a, a well-correlated indicator of phytoplankton biomass abundance and eutrophication, was estimated using ordinary least squares linear regression to calibrate surface reflectance with chl-a concentrations. Temporal gaps between sample and image acquisition were considered, and atmospheric correction dedicated to water surfaces was implemented using ACOLITE and those specific to each satellite platform. The developed models achieved determination coefficients higher than 0.69 with mean square errors close to 3 mg/m<sup>3</sup> for water bodies with low turbidity. Furthermore, the time series described by the models portray the seasonal variations in the lakes water bodies.

**Keywords:** water quality; remote sensing; machine learning; ACOLITE



**Citation:** Laneve, G.; Téllez, A.; Kallikkattil Kuruvila, A.; Bruno, M.; Messineo, V. Eutrophication and HAB Occurrence Control in Lakes of Different Origins: A Multi-Source Remote Sensing Detection Strategy. *Remote Sens.* **2024**, *16*, 1792. <https://doi.org/10.3390/rs16101792>

Academic Editor: Raphael M. Kudela

Received: 15 April 2024

Revised: 7 May 2024

Accepted: 16 May 2024

Published: 18 May 2024



**Copyright:** © 2024 by the authors. Licensee MDPI, Basel, Switzerland. This article is an open access article distributed under the terms and conditions of the Creative Commons Attribution (CC BY) license (<https://creativecommons.org/licenses/by/4.0/>).

## 1. Introduction

Remote sensing technologies have transformed perspectives in natural resource management, with the widespread utilization of remotely sensed data across diverse ecological disciplines in recent years [1,2]. Remote sensing (RS) plays an increasingly important role in identification of ecosystem progressive degradation and even in the success of recovery management [3]. In waterbodies the key factors and thresholds are a basal requirement to establish a remote sensing alert system in order to predict occurrence of superficial blooms [4].

The satellite Sentinel-2 is part of the European Copernicus Programme and provides optical remote sensing data with a space–time resolution of 13 spectral channels, able to detect chlorophyll a (chl-a) concentration and turbidity measure, two precious water quality indicators. Sentinel-2 has a very wide potential for remote sensing of inland waters, because it combines the high spatial resolution of conventional space-based sensors (i.e., Landsat and SPOT) with the higher time and spectral resolutions required for water surfaces. Since 2015, Sentinel-2 data has provided novel perspectives on water quality monitoring for smaller inland water bodies [5].

Several studies have shown their satellite ability in water quality monitoring [6–8], particularly using the bands near 750 nm, which solves the reflectance secondary peak related to pigment concentrations [9].

Moreover, Sentinel-2 has been utilized for identifying oil spills in both marine and freshwater settings [10,11], and several similar studies with other optical sensors are available, too [12–14].

Magnitude and frequency of phytoplankton blooms have increased globally in recent decades, as shown in data from ocean-color sensors on board satellites. Worldwide freshwater data show the same growing trend, and in this frame, phytoplankton biomass and chl-a concentration measurements are common methods in the study of water bodies' ecological status [15,16], because chl-a correlates well with phytoplankton biomass abundance [15,17], and it is used as a eutrophy indicator.

Remote sensing offers a means to predict chl-a levels through empirical models correlating visible and near infrared light reflection with lab-measured chl-a quantities [18]. Such predictions not only aid in assessing eutrophication severity but also significantly enhance detection, monitoring, and management of harmful algal blooms (HABs). Innovations in data analysis, such as algorithms that predict bloom occurrences, can also play a vital role in early warning systems and help policymakers and water managers to update guidelines, policies, and management strategies.

The trophic state of Lake Ladoga, the largest European lake with a 7765 km<sup>2</sup> surface, located in Finland, was successfully studied during years 1997–2019 using Copernicus Marine Environmental Monitoring Service (CMEMS) and GlobColour-merged chlorophyll-a OC5 (GlobColour CHL-OC5) satellite observations with algorithm OC5 [19]. Chl-a data derived from the satellite sensors SeaWiFS, MERIS, MODIS Aqua, VIIR, and OLCI (1997–2019) were used to define the chl-a general trend in Lake Ladoga.

In China, too, ecological remediation has gone on to become a national strategic project and a meaningful way to realize the construction of ecological civilization. A very recent work by Zhai et al. (2022) [20], based on RS technology with its short detection time, wide monitoring range, and high spatial resolution advantages, proposes RS evaluation as a watershed in the objective of ecological restoration, in order to monitor the improving effect of ecological remediation engineering and technically verify the reaching of targets set out before restoration. In a study on remediation effects in the Yongding River Basin in the Beijing region, images from satellites ZY-3 1 and 2 and Landsat were used from 2015 to 2020.

Based on these data, changes in eight hydric resources, water ecology, and ecological function indicators of the study area were calculated, in order to assess the effects of the ecological restoration engineering plan.

Additionally, RS provides time series of observations: there are available data from the Landsat (since 1972) and MODIS (since 2000) satellites, and the use of geostatistic analyses of remote sensing data allows for the production of historical pictures of lake conditions. In recent years, RS technologies have been applied in lake monitoring, in water quality assessment, and in lake evolution [21–24].

In this framing, the use of RS may help territorial managers and professionals to identify restoration priority areas and existing and emerging threats for restoration, to define restoration targets, and, finally, to track progress. [25].

In this study, we have employed ordinary least squares (OLS) linear regression, a widely adopted machine learning methodology in the field of remote sensing [26]. The study aims to develop regression models for the four lakes, using OLS linear regression to facilitate continuous monitoring and better understand the ecological changes occurring in these water bodies. By employing OLS regression, we have established a linear model that correlates the observed field data with remote sensing inputs, enabling the prediction of chlorophyll-a levels based on the remote sensing data.

The models generated using OLS regression were applied to the study of four volcanic and tectonic lakes in Central Italy, the trophic state of which worsened within thirty years from oligotrophy to eutrophy.

By compiling time series field data from 2005 to 2019, examining the chl-a concentration in the lakes, we aimed to correlate these measurements with ecological changes

observed in the lakes using continuous remote sensing image collection. This integration of machine learning algorithms with long-term ecological monitoring provides valuable insights into the dynamics of lake ecosystems and the impacts of eutrophication.

## 2. Materials and Methods

### 2.1. Study Sites

Lake Vico is an extended volcanic basin inside a crater depression of the Cimino Volcano Complex, 60 km north of Rome, Central Italy as shown in Figure 1. The surface is 12.09 km<sup>2</sup>, the volume is 260.7 m<sup>3</sup> × 10<sup>6</sup>, and the depth reaches 48.5 m (mean depth 21.6 m); the total turnover time is 17 years [27]. The total catchment area is 41 km<sup>2</sup>. The lake is part of a regional wildlife park and listed as a wetland of international importance by the Ramsar Convention. The vicinities of Lake Vico host extended hazel woods; some paper mills were located near the lake beginning in the year 1300, going out of business between 1963 and 1964. The lake is a drinking water reservoir for 10,000 people in two towns, Ronciglione and Caprarola, and a recreational area throughout the year.

Progressive eutrophication of the lake was established over the past several decades [27–31]. Anthropogenic activities like monocultural agriculture, industrial enterprises (pulp and paper mills), and wastewater discharges from civilian settlements caused a progressive increase in Lake Vico's trophic status [29,31,32], leading to the development of winter cyanobacterial toxic blooms of the red species *Planktothrix rubescens*.

Lake Albano is a volcanic basin inside a crater depression with an ellipsoid shape [33]. The lake's perimeter is 12 km, and its depth reaches 175 m. The mean renewal time is more than 67 years. Lacking outlet tributaries, the lake is characterized by an ancient Roman channel carved in the lava rocks through the crater, which was used to regulate the lake level. The lake is eutrophic due to human activities, which in the past caused development of algal blooms; the first evidence of this was highlighted by Cannicci (1954) [34]. Since 1960, due to uncontrolled water removal for human uses, the lake level lowered almost four meters under the artificial outflow, leading to a change from an oligotrophic condition to an eutrophic one.

Lake Trasimeno is a tectonic lake in the province of Perugia, Umbria. With an area of 128 km<sup>2</sup>, it is the largest lake in central Italy; this extension is flanked, however, by a shallow depth (average 4.3 m, maximum 6 m), which makes it classified as a laminar lake. Lake Trasimeno has no natural emissaries. The area of the basin catchment that drains into the lake is just 2.2 times larger than the lacustrine area. For these reasons, Trasimeno is characterized by a marked variability of water levels and volume stored, tightly bound to the variability of precipitation. The renewal time is 8–9 years. The lake ecosystem is of exceptional value for its wealth of flora and fauna. Tourism, agriculture, and livestock are the most important activities of the Trasimeno area. Until 1990, phytoplanktonic communities were mainly dominated by populations of chlorophyceae or diatoms while among the few cyanophyceae present were mainly *Phormidium* spp. and *Oscillatoria tenuis*. Subsequently, the community tended to be increasingly enriched with filamentous blue algae in the late summer, up to the manifestation of real explosions of *Cylindrospermopsis raciborskii* and *Planktothrix agardii*, throughout the depth of the lake. In the summer months of 2004 and 2005, there were intense blooms of *Cylindrospermopsis raciborskii*, even at great depths, following the presence of optimal conditions for the growth of blue algae, such as high water temperature, prolonged lighting and exaltation of eutrophic phenomena.

Lake Bolsena has an almost round shape typical for its origin, two islands, and an emissary river, a total area of 113.5 km<sup>2</sup> (fifth in Italy); it is located at 305 m., with a maximum depth of 151 m and an average depth of 81 m.

The theoretical water exchange time has been estimated at 120 years; actually the residence time of the waters in the lake is prolonged due to the difficulty with which the deep waters reach the emissary in summer as a result of the thermal stratification of the waters. Lately it has emerged that, due to the significant withdrawals, both from

the lake and from the aquifer, the flow rate of the emissary has halved, and therefore the replacement time has doubled.

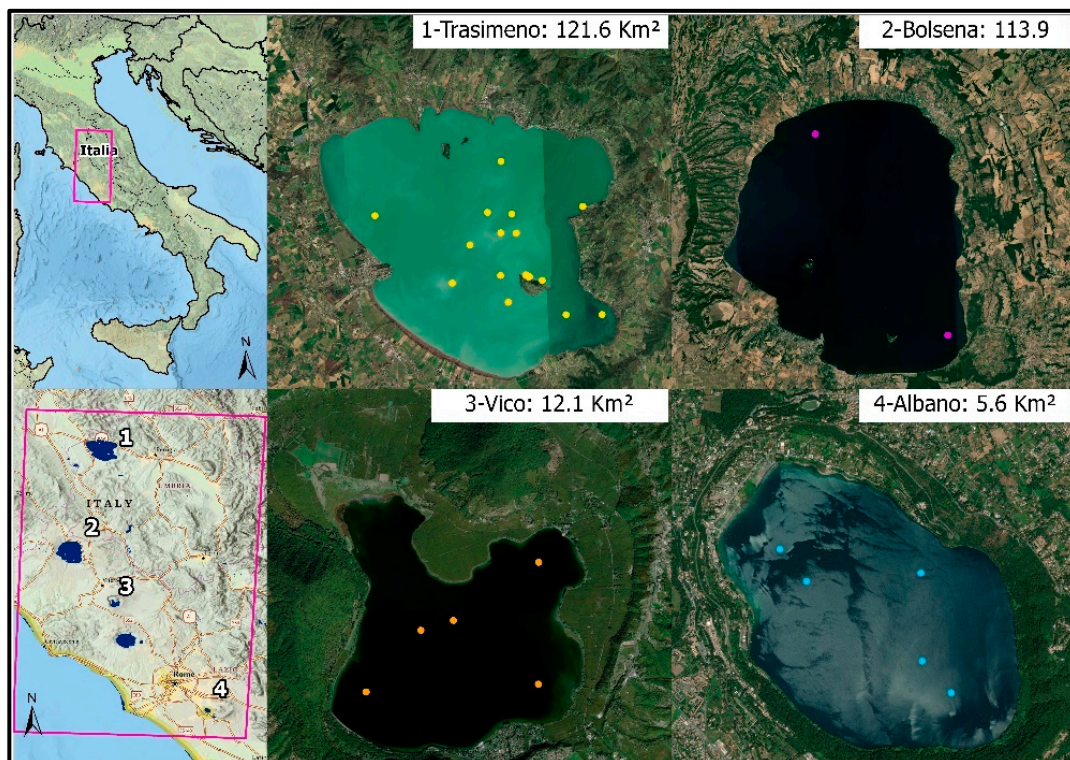


**Figure 1.** Study area with in situ samples according to Sentinel 2.

## 2.2. Water Sampling

Water samplings were carried out in Lake Vico every month from March 2018 to December 2019 and in Lake Albano from March 2018 to May 2019 in five surface stations; in Lake Bolsena from April 2019 to October 2019 in two central surface stations, and in Lake Trasimeno from July 2019 to December 2019 in one central surface station (Figure 1).

Water samples (1 L in volume) were collected using a 2.5 L Ruttner bottle by filling 1 L Pyrex glass bottles. The samples were stored in ice chests and transported to the laboratory. For microscopic observations, subsamples were analyzed by an inverted microscope (Leitz Labovert FS), according to Utermöhl (1931) [35] and Lund et al. (1958) [36], using 25 mL sedimentation chambers for phytoplankton identification and cell density estimation.

This study also integrates the GLORIA database, a globally representative hyperspectral in situ dataset for optical sensing of water quality, due to the limited presence of chlorophyll samples in Lake Trasimeno [37].

## 2.3. Chemical and Physical Parameters

Temperature, conductivity, dissolved oxygen, and pH were measured in the field, using a multiparametric probe (Mettler Toledo InLab1781, Milano, Italy) as in [32]. Chlorophyll a content was measured in 90% acetone/H<sub>2</sub>O-extracted samples according to SCOR/UNESCO method (1966) [38], using a Lambda Bio spectrophotometer (Perkin Elmer, Shelton, CT, USA).

## 2.4. Remote Sensing Detection

For the calibration of empirical models of chl-a by remote sensing, two satellite missions widely used for the estimation of water quality parameters were selected, which have high spatial resolution for sampling inland water bodies and a historical catalog sufficiently extensive to estimate time series [39,40]. The first one is Landsat with its platforms 5, 7, and

8, with a spatial resolution of 30 m and a revisit time of 16 days; the second one is Sentinel-2 with its platforms 2A and 2B with a spatial resolution of 10, 20, and 60 m depending on the band number, with a revisit time of 5 days. For this study, the VIS and NIR bands of both missions were selected.

To access the atmospherically corrected surface reflectance satellite products, the Planetary Computer catalog API was used to provide level 2A atmospherically corrected Sen2Cor images for Sentinel-2 and Landsat collection 2 with level 2 and LaSRC atmospheric correction (platforms 8–9)/LEDAPS (platforms 5–7). Image access and query was managed with the SpatioTemporal Asset Catalogs (STAC) standard.

Atmospheric correction is crucial in remote sensing applications to interpret satellite imagery, particularly in aquatic environments where atmospheric effects can distort the signal. In this research, we have chosen to utilize the ACOLITE atmospheric correction method, which is based on the dark spectrum fitting (DSF) algorithm [41].

To ensure optimal performance of the ACOLITE atmospheric correction, we followed recommended guidelines by setting up a region of interest (ROI) using a polygon. To perform atmospheric correction using ACOLITE, images from Sentinel-2 L1C and Landsat Level 1 Collection 2 were downloaded from the Copernicus browser and Earth Explorer platform. These images were then processed using ACOLITE to generate surface reflectances. ACOLITE is suitable for processing turbid waters and small inland water bodies but can also give satisfactory results for clearer waters and terrestrial environments [42].

Once the images were downloaded and processed, the spectral responses of each of the chlorophyll samples were extracted. Since water bodies are dynamic systems, with the capacity to modify their spectral characteristics as a consequence of aquatic currents, the calibration of water quality models should take into account images preferably acquired on the same day of in situ sampling; however, due to the limitations of the temporal resolution of each satellite mission, it is necessary to define temporal windows that adjust to the revisit time of each mission. In the case of Sentinel-2, a temporal window of two days before or after field sampling was selected, prioritizing images without contamination by clouds, shadows, or solar reflections. Of the 41 images, 30 matched the sampling date, 4 differed by 1 day, and 7 differed by two days. Due to its temporal resolution of 16 days, Landsat uses a temporal window of 4 days around the sampling date. Of the 24 images, 5 matched the sampling date, 8 differed by 1 day, 5 differed by 2 days, and 6 differed by 3 days. Figure 2 summarizes the process described for the extraction of spectral information.

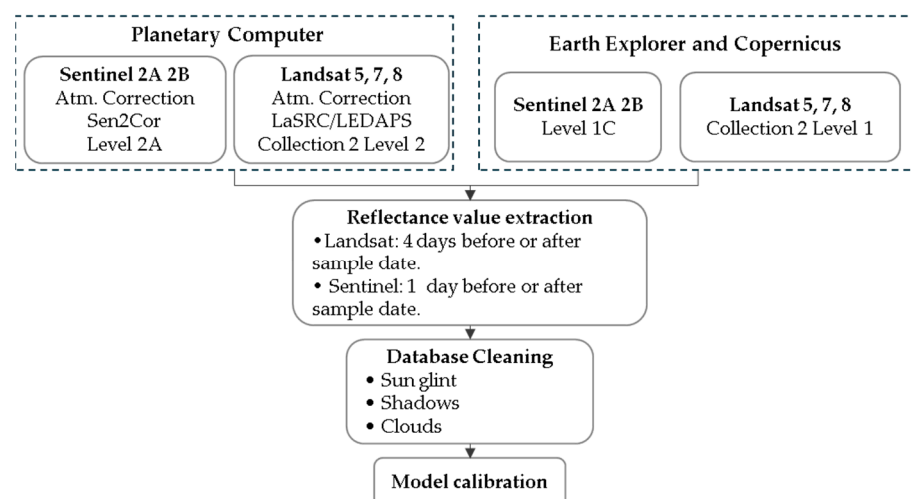


Figure 2. Flowchart of Sentinel-2 and Landsat image processing.

OLS regression estimates the relationship between independent variables (Sentinel-2 and Landsat bands) and a dependent variable (in situ chl-*a*), as described in the equation below:

$$y = b_0 + b_1 * x_1 + e$$

where:  $y$  = dependent variable (in situ chl-*a*)

$b_0$  = intercept

$b_1$  = coefficients

$x_1$  = independent variable (Sentinel-2/Landsat bands)

$e$  = error term

The basic premise of OLS linear regression is to minimize the sum of squared differences between the observed and predicted chlorophyll concentrations. This optimization process involves estimating the coefficients of the regression equation that minimize residual errors, thereby yielding the best-fitting line through the data points. In this study, ordinary least squares (OLS) simple linear regression was utilized for modeling, employing a set of more than 15 algorithms as predictor variables [43–48]. These algorithms include spectral index band ratios and models such as ocean color 2 and 3 (OC-2,3) [49]. Table 1 shows the most relevant ones according to their coefficient of determination ( $R^2$ ). Chlorophyll-*a* estimation algorithms were selected based on the optimal settings for the coefficient of determination and root mean square error (RMSE). In addition, due to the lack of a large number of samples, the consistency that each model manages to estimate spatially and temporally was considered by validating the historical series with in situ data. With the exception of Lake Albano, which was processed with Sentinel-2, the algorithms obtained for each of the 4 lakes were able to generalize the seasonal patterns of chlorophyll-*a*, so that it was possible to describe their historical behavior.

**Table 1.** Algorithms for chl-*a*.

Algorithm	Equation	Reference
Jaelani	$0.9889 (\text{red}/\text{NIR5}) - 0.3619$	[43]
Empirical (MSI)	$\text{NIR5} - (\text{red} + \text{NIR6})/2$	[44]
FLH Violet	$\text{green} - (\text{red} + \text{blue} - \text{red})$	[45]
Band Ratio 1	$1.1116 (\text{NIR5}/\text{blue}) + 0.7016$	[46]
Band Ratio 2	$\text{blue}/\text{green}$	[47]
Band Ratio 3	$\text{red}/\text{blue}$	[47]
Band Ratio 4	$\text{red}/\text{green}$	[48]

### 3. Results

#### 3.1. Chlorophyll-*a* Field Values

To obtain an appropriate comparison of RS and field chl-*a* values, only surface stations data were considered. Chl-*a* Vico surface values detected ranged from a minimum of 2.89  $\mu\text{g}/\text{L}$  (April 2019) to a maximum of 81.37  $\mu\text{g}/\text{L}$  (Ultima Spiaggia, December 2019); the average value was 15.07  $\mu\text{g}/\text{L}$ . In addition to the field values from the 2019 sampling activities, chl-*a* data from a 2005–2007 Vico study was used [31].

Chl-*a* Albano values went from a maximum of 21.59  $\mu\text{g}/\text{L}$ , February 2019, to a minimum of 1.04  $\mu\text{g}/\text{L}$ , May 2019, in addition to the field values of a 2001–2005 Albano study [50]. In both lakes, Albano and Vico, the highest values of chlorophyll-*a* were detected in the coldest months, corresponding to the period of maximum bloom of the toxic cyanobacteria *Planktothrix rubescens*.

Trasimeno Lake values went from a maximum value of 37.3  $\mu\text{g}/\text{L}$ , October 2019, to a minimum of 8.11  $\mu\text{g}/\text{L}$ , July 2019. Lake Bolsena went from a maximum value of 5.68  $\mu\text{g}/\text{L}$ , September 2019, to a minimum of 1.24  $\mu\text{g}/\text{L}$ , July 2019. The rather low values of chlorophyll *a* in this lake reflect its trophic status, which is much better than the other lakes studied.

Field data were compared to RS detections, in order to achieve a broader view of the chl-*a* trend in the Lake Vico during a fourteen-year period. The 2005 chl-*a* mean field

value was 2.54 µg/L, (max. value 5.5 µg/L; December, Fogliano); the 2006 mean value was 3.76 µg/L, (max. value 10.04 µg/L; February, lake center); the 2007 mean value was 3.87 µg/L, (max. value 4.86 µg/L; February, Bella Venere).

The general trend of chl-*a* mean surface concentration in Lake Vico over a fourteen-year period was positive, following an exponential curve ( $R^2 = 0.91$ ). The single sampling stations showed similar positive trends, considering the seasonal bloom period ( $R^2$  from 0.68, Bella Venere station, to 0.91, Ultima Spiaggia station; Figure 3).

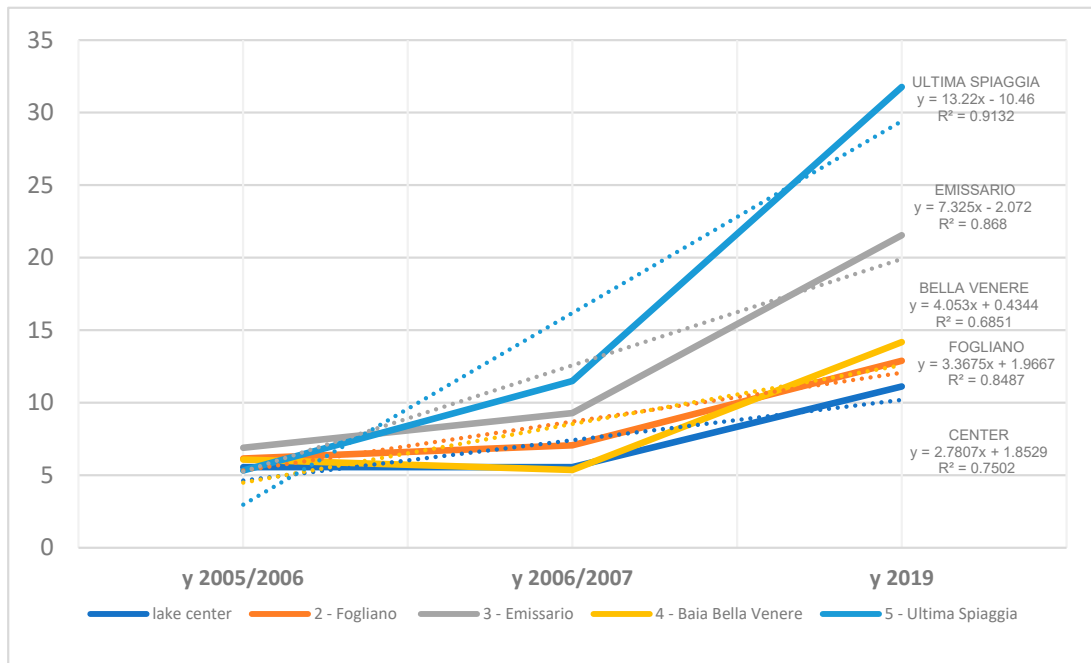


**Figure 3.** Seasonal (Nov.-Mar.) chl-*a* average in the five superficial Vico stations with their regression lines, trend lines and values.

The microcystin and BMAA seasonal presence, detected using an ELISA immunoassay [51], in Vico and Albano (Figure 4, 2018–2019 years) showed a high correlation coefficient ( $R^2 = 0.97$ ), confirming a production due to cyanobacterial blooms, mainly composed of *Planktothrix rubescens*.

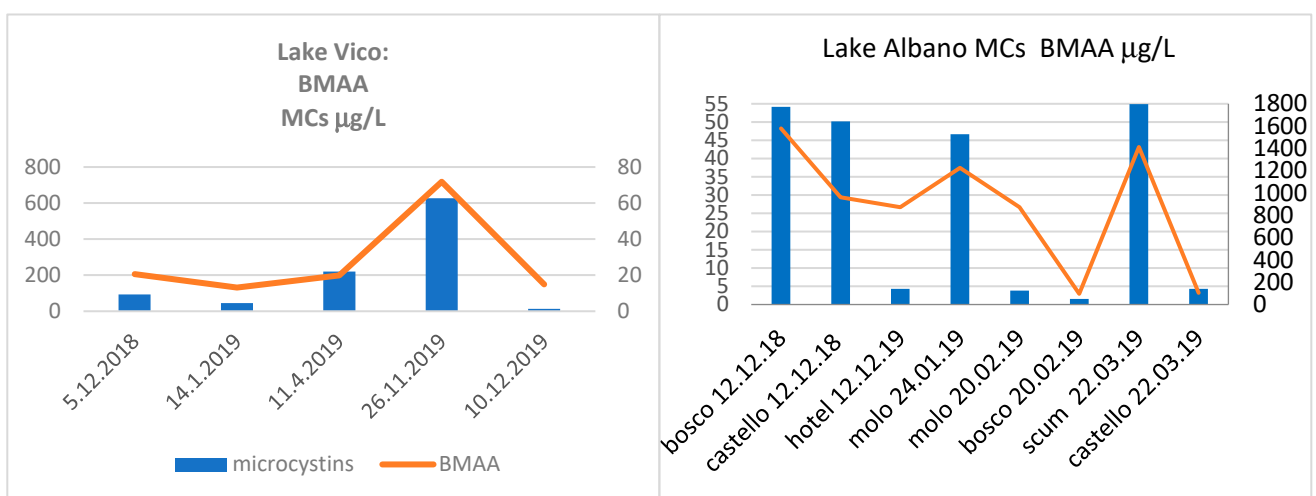


**Figure 4.** BMAA vs. microcystins concentration (µg/L) in lakes Vico and Albano.

### 3.2. Remote Sensing Detection

Tables 2 and 3 show the best empirical models obtained for the Sen2Cor, LaSRC/LEDAPS, and ACOLITE atmospheric corrections. Among the models obtained, band ratios widely used for remote sensing of water bodies with low chlorophyll concentrations, around  $5 \text{ mg/m}^3$ , and turbidity conditions that do not significantly compromise the detection of chl-*a* are identified, as is the case of “B/G” or the “R/G” that take advantage of the peak reflectance in the green region and the absorptions in the blue and red regions. In the case of the Jaelani, empirical, and band ratio 1 algorithms, these incorporate near-infrared bands, which can help in the detection of chlorophyll in environments with higher levels of turbidity, as is the case of Trasimeno.

**Table 2.** Sentinel-2 algorithms for chl-*a*, with atmospheric correction Sen2Cor and ACOLITE.

Lake	Atm. Correction	Sentinel-2					
		x	Models	N	Range $\text{mg/m}^3$	R <sup>2</sup>	RMSE
Albano	ACOLITE	B/G	$-8.7 + (28.9 \times x)$	10	1–22	0.69	2.7
	Sen2cor	B/G	$-25.6 + (46.9 \times x)$	10	1–22	0.57	3.1
Vico	ACOLITE	Band Ratio 1	$-9.3 + (15.6 \times x)$	7	1–23	0.76	3.1
	Sen2cor	Band Ratio 1	$-26.5 + (29.5 \times x)$	8	1–23	0.76	3.12
Bolsena	ACOLITE	Empirical	$3.32 + (-795.5 \times x)$	7	1–6	0.72	0.7
	Sen2cor	R/B	$0.18 + (11.15 \times x)$	7	1–6	0.68	0.74
Trasimeno	ACOLITE	Empirical	$1.47 + (1127.7 \times x)$	16	1–37	0.72	6.8
	Sen2cor	Empirical	$-0.32 + (1186.2 \times x)$	16	1–37	0.76	6.4

**Table 3.** Landsat algorithms for chl-*a*, with ACOLITE and LaSRC/LEDAPS atmospheric correction.

Lake	Atm. Correction	Landsat					
		x	Models	N	Range $\text{mg/m}^3$	R <sup>2</sup>	RMSE
Albano	ACOLITE	R/G	$-26.296 + (68.67 \times x)$	10	1–11	0.86	1.2
	LaSRC/LEDAPS	FLH Violet	$3.45 + (465.008 \times x)$	10	1–11	0.56	2.23
Vico	ACOLITE	Jaelani	$1.75 + (8.047 \times x)$	14	0.8–14.3	0.79	1.9
	LaSRC/LEDAPS	Jaelani	$0.681 + (7.45 \times x)$	14	0.8–14.3	0.56	2.7

Overall, the empirical algorithms obtained exhibit coefficients of determination close to 0.71, with RMSE values ranging from 0.7 to  $6.8 \text{ mg/m}^3$ . Both ACOLITE and Sen2Cor have demonstrated similar performance when evaluating correlation coefficients and root mean square errors between homologous models. For the case of Lake Vico and Sentinel-2, the band ratio 1 model obtained the best coefficient for both atmospheric corrections with very close R<sup>2</sup> and RMSE values.

Due to the small number of samples available for Bolsena and Trasimeno, it was not possible to develop models for Landsat; however, the models obtained with Sentinel-2 achieved determination coefficients of 0.72 and 0.76, respectively. In Vico, the Jaelani model obtained with Landsat data achieved the best results, with a difference of 0.23 between the determination coefficients, with ACOLITE being the best performing.

Although for Lake Albano, the empirical Sentinel-2 models achieve coefficients of determination of 0.58 and 0.69 for Sen2Cor and ACOLITE, respectively, a lack of temporal consistency in chlorophyll-*a* levels has been observed. When reviewing the spectral signatures of each sample with its concentration, an inverse relationship was found. In other words, the peak green reflectance of higher concentrations of chl-*a* should be higher than that of lower concentrations; however, in the case of Lake Albano, the opposite behavior is

present, which could be explained by the predominance of red pigments associated with the species *Planktothrix rubescens* which blooms during the winter period. [52]; however, when analyzing indices with bands in the red, it was not possible to obtain coefficients of determination higher than 0.37. Since such behavior was not found to be so strongly marked in Landsat, it was possible to develop an empirical model for this platform.

When relating the 1:1 slope to the regression line obtained for each model using the Sen2Cor and LaSRC/LEDAPS atmospheric corrections (Figure 5), two distinctive patterns are observed. First, an overestimation of chlorophyll-*a* is evident when concentrations are lower. In the cases of Vico, Albano, Bolsena, and Trasimeno, the overestimation ranges around 2.5, 2, 1, and 2.5  $\text{mg}/\text{m}^3$ , respectively. Secondly, an underestimation of chlorophyll-*a* concentrations is detected when the sampled values are higher. For Lake Vico, the underestimation is around 3.5  $\text{mg}/\text{m}^3$ , while for Albano, Bolsena, and Trasimeno, the values are around 2.8, 1, and 8  $\text{mg}/\text{m}^3$ , respectively.

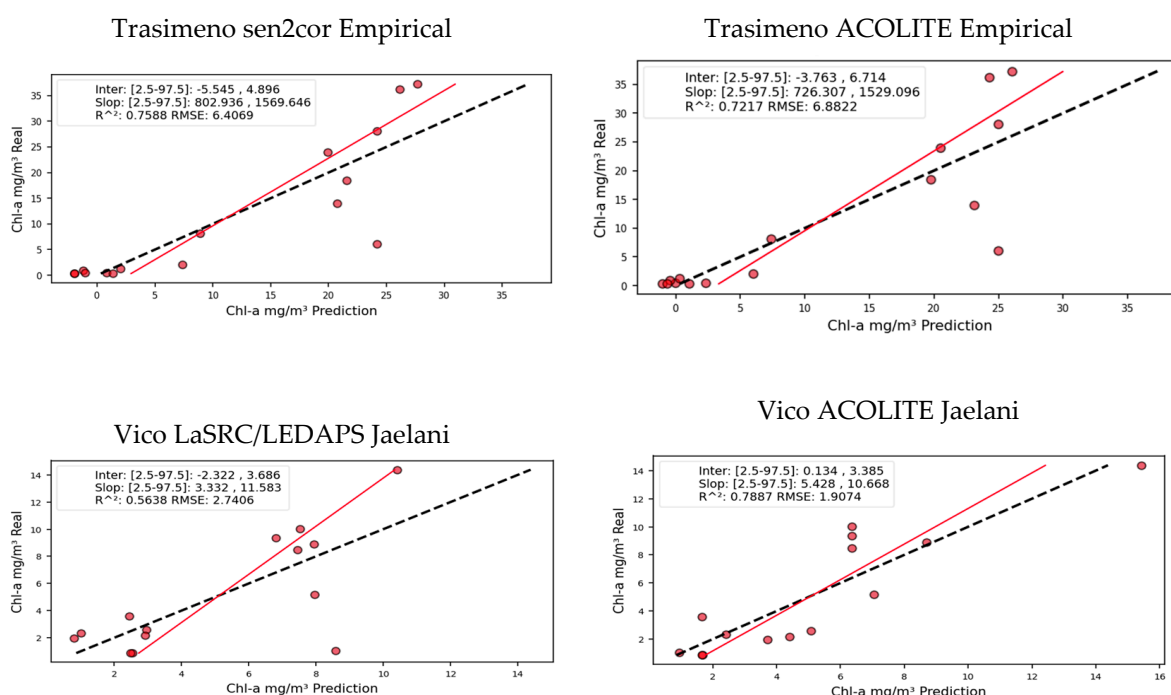


**Figure 5.** Scatter plot, estimated chl-*a* values vs. in situ values.

Figure 6 shows the historical series of chl-*a* concentration for the 4 lakes; the series was constructed with Sentinel-2 and Landsat images processed with the Sen2Cor and LaSRC atmospheric correction algorithms. With the exception of the Albano model processed with Sentinel-2, which presents inconsistency in the chl-*a* estimation, the models describe a seasonal behavior. Some plots present outliers of chl-*a* as a consequence of cloudiness or shadows. Of the studied lakes, Trasimeno presents the highest chl-*a* concentrations, with a strongly marked seasonality with maxima that can reach 40  $\text{mg}/\text{m}^3$ , followed by Vico with concentrations close to 25  $\text{mg}/\text{m}^3$ , Albano with 20  $\text{mg}/\text{m}^3$ , and Bolsena with 10  $\text{mg}/\text{m}^3$ .

For Trasimeno, the average chlorophyll concentrations for autumn reach 19  $\text{mg}/\text{m}^3$  with a standard deviation of 7.9; from this point the concentrations decrease until reaching their minimums in the months of May, with average concentrations of 3.8  $\text{mg}/\text{m}^3$ . Bolsena, on the other hand, maintains much more homogeneous concentrations during the year, with an increase in its concentrations for the month of August and a progressive decrease until the month of January; in general, Bolsena maintains constant cycles without a clear trend in the increase of its concentrations, according to the absence of important cyanobacterial blooms in the lake and its oligo-mestrophic state.

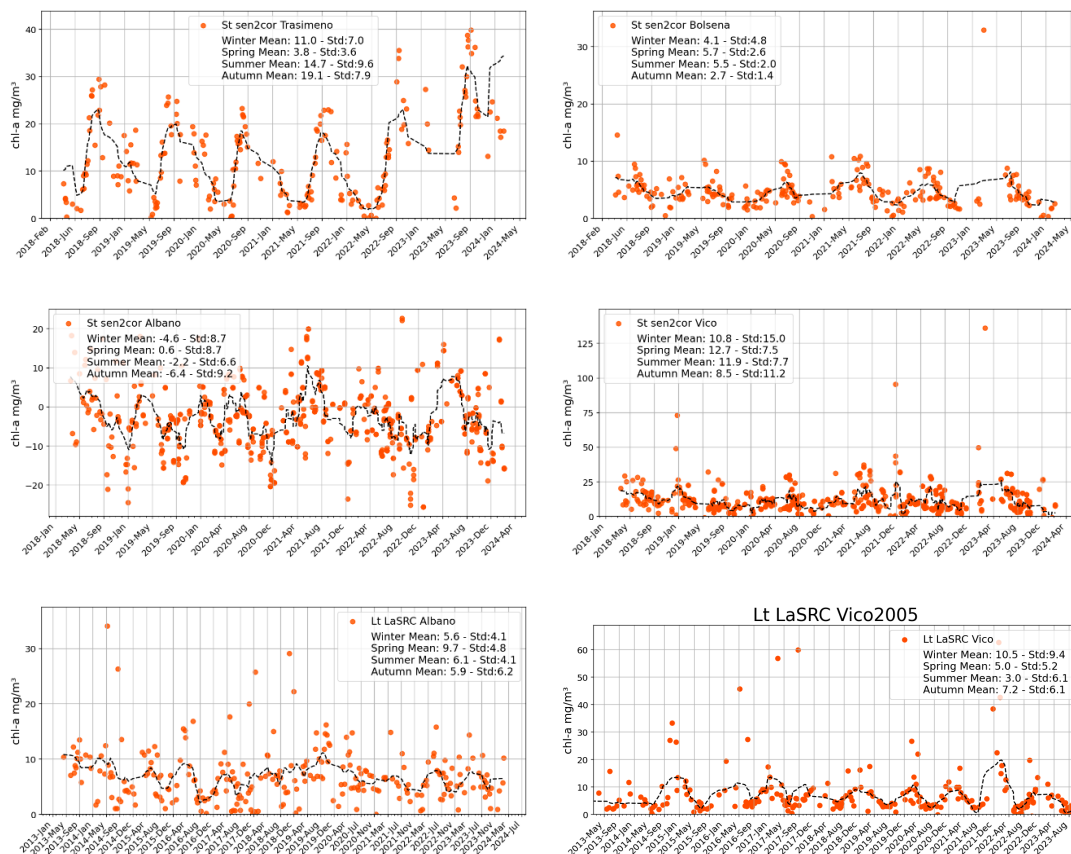


**Figure 6.** Time series of chl-*a* for Trasimeno, Bolsena, Albano, and Vico lakes.

The high dispersion in chl-*a* concentrations in Albano is mainly due to noise introduced in the images as a result of the presence of clouds or shadows that could not be masked by the SCL. Having a historical series with inconsistencies limits the work of distinguishing clear seasonal patterns in chl-*a*; however, it is possible to observe a possible cycle, with an increase in chl-*a* from the beginning of February to the end of April, followed by a decrease until the end of August.

Although a direct comparison between sensors is not the most appropriate without harmonization, Figure 7 presents the historical series of chl-*a* between the algorithms developed in Lake Vico for the Sentinel-2 and Landsat missions, the lack of Landsat data makes it difficult to compare seasonality between series. Although in some periods a correspondence is perceived, it is not possible to conclude that both series have similar cycles. On the other hand, both missions share the same range of chl-*a* concentrations.

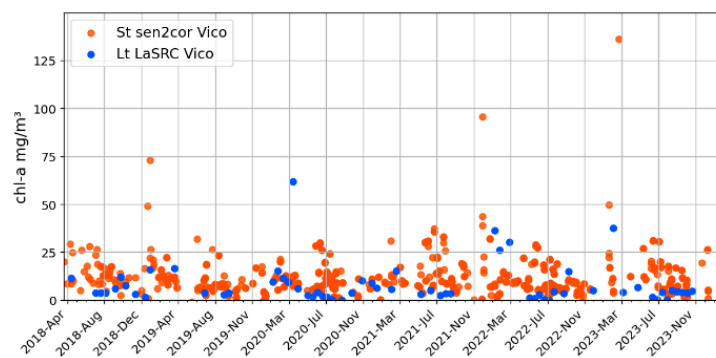


**Figure 7.** Landsat and Sentinel 2 historical series.

#### 4. Discussion

The anthropogenic activities of the settlements around Lake Vico, particularly the extended and abundantly fertilized hazelnut monoculture, could be the sources for nutrients driving algal blooms through watershed run-off and, more extensively, polluted groundwaters [31]. In general, phosphorus compounds arrive at superficial waters through leaching of fertilizers, human and animal excrements, and/or detergents and cleansing products. Depending on the concentration of phosphates in the water, eutrophication can occur in waterbodies, phosphorus (the “limiting nutrient”) controlling the pace at which algae and aquatic plants are produced. Despite the end of the paper mill activity, the nutrient level in the lake has progressively growing, mainly due to the fertilizations of the extending hazelnut crops on the lake watershed. This increase favoured eutrophy and the onset of seasonal blooms by several cyanobacterial species in the lake, mainly the toxic *P. rubescens* during the autumn and winter months.

The pulsating attitude showed by the temporal chl-*a* trend of Sentinel data, and much longer, of Landsat data has been observed in other lakes, concerning investigations through several decades [19]. Recent studies propose a possible reason of this in the consequences of uneven or incomplete annual mixings and the following differences in stratification dynamics and irradiance on phytoplanktonic populations [53]. The need to determine a reliable correspondence between RS and field chl-*a* values shows its importance, in the case of Lake Vico and Albano, for the strong correlation in lake waters between toxin levels and the cold season (Figure 4). Regarding Lake Albano, the general trend of the population dynamics for *P. rubescens* in the lake shows superficial stratification with blooms in winter and metalimnic stratification with a peak (25–30 m) in summer, but nevertheless with an overall population decrease (80–86%) in the late April to early November period. These situates Albano in state of mesotrophy tending to eutrophy caused by the increasing levels of N and P from manure treatment and sewage inputs in the groundwater feeding the lake and in the lakewater itself. Contaminant concentration resulting from the progressive decrease of the water lake level, which occurred over decades of uncontrolled drainage in groundwaters, presumably helped this process.

Although each lake has specific optical properties, by comparing the spectral response of each lake with previous optical water type works [54,55] it is possible to distinguish Trasimeno as a high turbidity lake with very different optical properties from the rest of the studied lakes, with the characteristic pattern of high reflectivity near the green and near infrared region, unlike Vico, Bolsena, and Albano with low reflectivity in these regions (Figure 8).

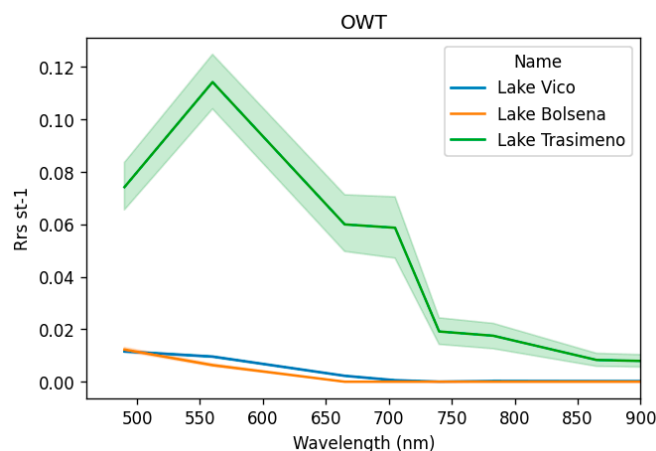


**Figure 8.** Optical water property estimate with Sentinel-2 images.

In situ chl-*a* data considered for generating the regression model was collected during the periods of February, June, and October 2006, as well as April and December 2019. Upon

comparing the seasonal dynamics of the time series for Lake Vico using the generated model, it was observed that the model successfully captured the general patterns of chl-*a* fluctuations, even in regions lacking in situ samples. This observation highlights a correspondence between the modeled data and the actual chl-*a* dynamics (Figure 9).

The seasonal dynamics of Trasimeno are consistent with studies that develop high-frequency monitoring through permanent stations for the generation of empirical models through reflectance; the studies conclude that the increase in chl-*a* concentrations are associated with heat waves and rainfall events, with a peak in the month of September, also finding an increase in the cyanobacterium *Cylindrospermopsis raciborskii* [40,56].

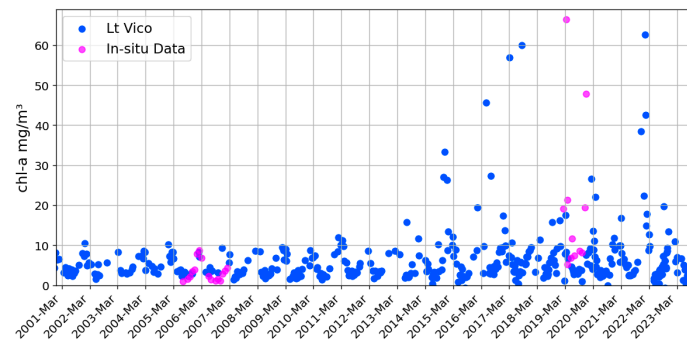


**Figure 9.** Temporal trends of chlorophyll-*a* concentrations: a comparative analysis of in situ and Landsat images.

## 5. Conclusions

In general, the best lake models maintain coefficients of determination above 0.69, with a root mean square error (RMSE) of about 3 mg/m<sup>3</sup> for lakes with low turbidity such as Vico, Albano, and Bolsena. However, in the case of Lake Trasimeno, this value rises to 6.6 mg/m<sup>3</sup>.

Except for Albano, whose data were affected by shadows and clouds, the historical series estimated with the OLS linear regression models managed to reflect seasonal behavior; differences were observed in the seasonal cycles of each of the lakes, possibly due to the different chlorophyll species found in each one.

In terms of reflectance, a generalized decrease was found for the images processed with ACOLITE, which can result in negative values when the surface reflectance of the water is close to 0; this can affect the calibration of models and consequently their performance. Both ACOLITE and Sen2cor and LaSRC/LEDAPS presented similar R<sup>2</sup> and RMSE; for our study, however, because of the number of samples used, it is not possible to conclude that any of the atmospheric corrections offer advantages over the other.

The four Italian lakes analysed in this study are a significant water resource for agricultural and recreational activities, as well as important protected areas, with a crucial role in the ecological balance: they provide indispensable habitats for diverse species of plants and animals, enriching biodiversity and supporting local economies through fishing and agriculture. They are also vital sources of drinking water and places for leisure and tourism. However, they face annual challenges of eutrophication and algal bloom occurrences due to excessive nutrient accumulation and lowering water levels due to excessive withdrawals. In general, efficient management of algal blooms necessitates a comprehensive analysis of their spatiotemporal distribution characteristics and an effective monitoring means that extensive and expensive sampling programs are needed. For aquatic environments, the fulfilment of the monitoring requirements is an acknowledged problem due to the size of the largest lakes, the enormous number of lakes in total, their considerable temporal and spatial variability and, in some cases, their inaccessibility. In addition, not all lakes are monitored because of lack of resources. The ecological status of a water body can be described by various biological and physical–chemical quality measurements, and several of these important ecological parameters can be monitored

from space, such as chlorophyll *a* concentration. Using RS detection to quantify chl-*a* values in lake for monitoring cyanobacterial blooms leads to a significantly improved spatial and temporal frequency of monitoring and forecasting and long-term cost savings. This study proposes suitable models to assess the presence of potentially toxic algal blooms through the RS quantification of chl-*a*. This could open up interesting prospects from an economic, health, and social point of view regarding the launch of further studies aimed at developing an effective system for monitoring cyanobacteria blooms in freshwater resources and marine environments.

**Author Contributions:** Conceptualization, M.B. and G.L.; methodology, M.B. and G.L.; formal analysis G.L., A.T., A.K.K. and V.M.; investigation, V.M., M.B., A.T. and A.K.K.; resources, A.T. and A.K.K.; data curation, M.B., G.L., A.T., A.K.K. and V.M. writing—original draft preparation, M.B., G.L., A.T., A.K.K. and V.M.; writing—review and editing, V.M. All authors have read and agreed to the published version of the manuscript.

**Funding:** This research received no external funding.

**Data Availability Statement:** The original contributions presented in the study are included in the article, further inquiries can be directed to the corresponding author.

**Conflicts of Interest:** The authors declare no conflicts of interest.

## References

1. Kumar, N.; Yamaç, S.S.; Velmurugan, A. Applications of remote sensing and GIS in natural resource management. *J. Andaman Sci. Assoc.* **2015**, *20*, 1–6.
2. Corbane, C.; Lang, S.; Pipkins, K.; Alleaume, S.; Deshayes, M.; Millán, V.E.G.; Strasser, T.; Borre, J.V.; Toon, S.; Michael, F. Remote sensing for mapping natural habitats and their conservation status—New opportunities and challenges. *Int. J. Appl. Earth Obs. Geoinf.* **2015**, *37*, 7–16. [[CrossRef](#)]
3. Cabello, J.; Fernández, N.; Alcaraz-Segura, D.; Oyonarte, C.; Piñeiro, G.; Altesor, A.; Delibes, M.; Paruelo, J. The ecosystem functioning dimension in conservation: Insights from remote sensing. *Biodivers. Conserv.* **2012**, *21*, 3287–3305. [[CrossRef](#)]
4. Khorasani, H.; Kerachian, R.; Malakpour-Estalaki, S. Developing a comprehensive framework for eutrophication management in off-stream artificial lakes. *J. Hydrol.* **2018**, *562*, 103–124. [[CrossRef](#)]
5. Drusch, M.; Del Bello, U.; Carlier, S.; Colin, O.; Fernandez, V.; Gascon, F.; Hoersch, B.; Isola, C.; Laberinti, P.; Martimort, P. Sentinel-2: ESA's optical high-resolution mission for GMES operational services. *Remote Sens. Environ.* **2012**, *120*, 25–36. [[CrossRef](#)]
6. Liu, H.; Li, Q.; Shi, T.; Hu, S.; Wu, G.; Zhou, Q. Application of Sentinel 2 MSI images to retrieve suspended particulate matter concentrations in Poyang Lake. *Remote Sens.* **2017**, *9*, 761. [[CrossRef](#)]
7. Pahlevan, N.; Sarkar, S.; Franz, B.; Balasubramanian, S.V.; He, J. Sentinel-2 MultiSpectral Instrument (MSI) data processing for aquatic science applications: Demonstrations and validations. *Remote Sens. Environ.* **2017**, *201*, 47–56. [[CrossRef](#)]
8. Toming, K.; Kutser, T.; Laas, A.; Sepp, M.; Paavel, B.; Nöges, T. First Experiences in Mapping Lake Water Quality Parameters with Sentinel-2 MSI Imagery. *Remote Sens.* **2016**, *8*, 640. [[CrossRef](#)]
9. Zhao, D.; Xing, X.; Liu, Y.; Yang, J.; Wang, L. The Relation of Chlorophyll- *a* Concentration with the Reflectance Peak near 700 Nm in Algae-Dominated Waters and Sensitivity of Fluorescence Algorithms for Detecting Algal Bloom. *Int. J. Remote Sens.* **2010**, *31*, 39–48. [[CrossRef](#)]
10. Kolokoussis, P.; Karathanassi, V. Oil Spill Detection and Mapping Using Sentinel 2 Imagery. *J. Mar. Sci. Eng.* **2018**, *6*, 4. [[CrossRef](#)]
11. Laneve, G.; Bruno, M.; Mukherjee, A.; Messineo, V.; Giuseppetti, R.; De Pace, R.; Magurano, F.; D'Ugo, E. Remote sensing detection of algal blooms in a lake impacted by petroleum hydrocarbons. *Remote Sens.* **2022**, *14*, 121. [[CrossRef](#)]
12. Bulgarelli, B.; Djavidnia, S. On MODIS retrieval of oil spill spectral properties in the marine environment. *IEEE Geosci. Remote Sens. Lett.* **2012**, *9*, 398–402. [[CrossRef](#)]
13. Zhao, J.; Temimi, M.; Ghedira, H.; Hu, C. Exploring the potential of optical remote sensing for oil spill detection in shallow coastal waters—a case study in the Arabian Gulf. *Opt. Express* **2014**, *22*, 13755. [[CrossRef](#)] [[PubMed](#)]
14. Luciani, R.; Laneve, G. Oil Spill Detection Using Optical Sensors: A Multi-Temporal Approach. *Satell. Oceanogr. Meteorol.* **2018**, *3*. [[CrossRef](#)]
15. Harvey, E.T.; Kratzer, S.; Philipson, P. Satellite-based water quality monitoring for improved spatial and temporal retrieval of chlorophyll-*a* in coastal waters. *Remote Sens. Environ.* **2015**, *158*, 417–430. [[CrossRef](#)]
16. Chen, S.; Meng, Y.; Lin, S.; Xi, J. Remote Sensing of the Seasonal and Interannual Variability of Surface Chlorophyll-*a* Concentration in the Northwest Pacific over the Past 23 Years (1997–2020). *Remote Sens.* **2022**, *14*, 5611. [[CrossRef](#)]
17. Marcelli, M.; Piermattei, V.; Madonia, A.; Mainardi, U. Design and application of new low-cost instruments for marine environmental research. *Sensors* **2014**, *14*, 23348–23364. [[CrossRef](#)] [[PubMed](#)]
18. Karetnikov, S.; Leppäranta, M.; Montonen, A. A time series of over 100 years of ice seasons on Lake Ladoga. *J. Great Lakes Res.* **2017**, *43*, 979–988. [[CrossRef](#)]

19. Gbagir, A.-M.G.; Colpaert, A. Assessing the trend of the trophic state of lake Ladoga based on multi-year (1997–2019) CMEMS globcolour-merged CHL-OC5 satellite observations. *Sensors* **2020**, *20*, 6881. [CrossRef]
20. Zhai, L.; Cheng, S.; Sang, H.; Xie, W.; Gan, L.; Wang, T. Remote sensing evaluation of ecological restoration engineering effect: A case study of the Yongding River watershed, China. *Ecol. Eng.* **2022**, *182*, 106724. [CrossRef]
21. Bouffard, D.; Kiefer, I.; Wüest, A.; Wunderle, S.; Odermatt, D. Are surface temperature and chlorophyll in a large deep lake related? An analysis based on satellite observations in synergy with hydrodynamic modelling and in-situ data. *Remote Sens. Environ.* **2018**, *209*, 510–523. [CrossRef]
22. Fichot, C.G.; Matsumoto Holt, K.B.; Gierach, M.M.; Tokos, K.S. Assessing change in the overturning trend of the Laurentian Great Lakes using remotely sensed lake surface water temperatures. *Remote Sens. Environ.* **2019**, *235*, 111427. [CrossRef]
23. Yao, F.F.; Wang, J.D.; Wang, C.; Crétaux, J.F. Constructing long-term high-frequency time series of global lake and reservoir areas using Landsat imagery. *Remote Sens. Environ.* **2019**, *232*, 111210. [CrossRef]
24. Zhang, G.Q.; Chen, W.F.; Li, G.; Yang, W.; Yi, S.; Luo, W. Lake water and glacier mass gains in the northwestern Tibetan Plateau observed from multi-sensor remote sensing data: Implication of an enhanced hydrological cycle. *Remote Sens. Environ.* **2020**, *237*, 111554. [CrossRef]
25. Cordell, S.; Questad, E.J.; Asner, G.P.; Kinney, K.M.; Thaxton, J.M.; Uowolo, A.; Brooks, S.; Chynoweth, M.W. Remote sensing for restoration planning: How the big picture can inform stakeholders. *Restor. Ecol.* **2017**, *25*, S147–S154. [CrossRef]
26. Escoto, J.E.; Blanco, A.C.; Argamosa, R.J.; Medina, J.M. Pasig river water quality estimation using an empirical ordinary least squares regression model of Sentinel 2 satellite images. *Int. Arch. Photogramm. Remote Sens. Spat. Inf. Sci.* **2021**, *46*, 161–168. [CrossRef]
27. Barbanti, L.; Carollo, A.; Libera, V. Carta batimetrica del Lago di Vico. In *Indagini Limnologiche sui Laghi di Bolsena, Bracciano, Vico e Trasimeno*; Series Quaderni dell'Istituto di Ricerca Sulle Acque, CNR, Eds.; CNR: Roma, Italia, 1974; Volume 17.
28. Gelosi, E. Classification of the ecological status of volcanic lakes in Central Italy. Available online: <https://www.semanticscholar.org/paper/Classification-of-the-ecological-status-of-volcanic-Margaritora-Bazzanti/e663484d5d2546f731628e30e7efbf26f6076444> (accessed on 15 May 2024).
29. Dyer, M. The water quality at Lago di Vico during 1992–1993. *Sci. Total Environ.* **1995**, *171*, 77–83. [CrossRef]
30. Franzoi, P.; Scialanca, F.; Castaldelli, G. Lago di Vico (Italia Centrale): Analisi delle principali variabili fisiche e chimiche delle acque in relazione all'evoluzione trofica. Available online: [https://www.semanticscholar.org/paper/Lago-di-Vico-\(Italia-Centrale\)-analisi-delle-e-in-Franzoi-Scialanca/b7f46a07d166cb40ee581eef98c704b84d695aa2](https://www.semanticscholar.org/paper/Lago-di-Vico-(Italia-Centrale)-analisi-delle-e-in-Franzoi-Scialanca/b7f46a07d166cb40ee581eef98c704b84d695aa2) (accessed on 15 May 2024).
31. Mazza, R.; Capelli, G.; Teoli, P.; Bruno, M.; Messineo, V.; Melchiorre, S.; Di Corcia, A. Toxin Contamination of Surface and Subsurface Water Bodies Connected with Lake Vicos Watershed (Central Italy). In *Drinking Water: Contamination, Toxicity and Treatment*; Romero, J.D., Molina, P.S., Eds.; Nova Publishers Inc.: New York, NY, USA, 2008; pp. 1–100.
32. Bruno, M.; Gallo, P.; Messineo, V.; Melchiorre, S. Health risk associated with microcystin presence in the environment: The case of an Italian Lake (Lake Vico, Central Italy). *Int. J. Environ. Prot.* **2012**, *2*, 34–41.
33. Chondrogianni, C.; Ariztegui, D.; Guilizzoni, P.; Lami, A. Lakes Albano and Nemi (central Italy): An overview. In *Palaeoenvironmental Analysis of Italian Crater Lakes and Adriatic Sediments (PALICLAS)*; Guilizzoni, P., Oldfield, F., Eds.; dell'Istituto Italiano di Idrobiologia: Pallanza, Italy, 1996; Volume 55, pp. 17–22.
34. Cannicci, G. Su una eccezionale fioritura del Lago di Albano. *Boll. Pesca Piscic. Idrobiol.* **1953**, *8*, 221–233.
35. Utermöhl, H. Neue Wege in der quantitativen Erfassung des Planktons (mit besonderer Berücksichtigung des Ultraplanktons). *Verh. Int. Ver. Theor. Angew. Limnol.* **1931**, *5*, 567–596.
36. Lund, J.W.G.; Kipling, C.; Le Cren, E. The inverted microscope method of estimating algal numbers and the statistical basis of estimations by counting. *Hydrobiology* **1958**, *11*, 143–170. [CrossRef]
37. Lehmann, M.K.; Gurlin, D.; Pahlevan, N.; Alikas, K.; Conroy, T.; Anstee, J.; Balasubramanian, S.V.; Barbosa, C.C.F.; Binding, C.; Bracher, A.; et al. GLORIA—A Globally Representative Hyperspectral in Situ Dataset for Optical Sensing of Water Quality. *Sci. Data* **2023**, *10*, 100. [CrossRef] [PubMed]
38. Group 17, SCOR Working. Determination of Photosynthetic Pigments in Sea-Water. 1966. Available online: <https://repository.oceanbestpractices.org/handle/11329/2339> (accessed on 15 May 2024).
39. Niroumand-Jadidi, M.; Bovolo, F.; Bresciani, M.; Gege, P.; Giardino, C. Water Quality Retrieval from Landsat-9 (OLI-2) Imagery and Comparison to Sentinel-2. *Remote Sens.* **2022**, *14*, 4596. [CrossRef]
40. Free, G.; Bresciani, M.; Pinardi, M.; Giardino, C.; Alikas, K.; Kangro, K.; Rõöm, E.-I.; Vaičiūtė, D.; Bučas, M.; Tiškus, E.; et al. Detecting Climate Driven Changes in Chlorophyll-a Using High Frequency Monitoring: The Impact of the 2019 European Heatwave in Three Contrasting Aquatic Systems. *Sensors* **2021**, *21*, 6242. [CrossRef] [PubMed]
41. Vanhellemont, Q. Adaptation of the Dark Spectrum Fitting Atmospheric Correction for Aquatic Applications of the Landsat and Sentinel-2 Archives. *Remote Sens. Environ.* **2019**, *225*, 175–192. [CrossRef]
42. Pahlevan, N.; Smith, B.; Schalles, J.; Binding, C.; Cao, Z.; Ma, R.; Alikas, K.; Kangro, K.; Gurlin, D.; Nguyen, H.; et al. Seamless retrievals of chlorophyll-a from Sentinel-2 (MSI) and Sentinel-3 (OLCI) in inland and coastal waters: A machine-learning approach. *Remote Sens. Environ.* **2020**, *240*, 111604. [CrossRef]
43. Darmawan, A.; Herawati, E.Y.; Azkiya, M.; Cahyani, R.N.; Aryani, S.H.; Fradaningtyas; Hardiyanti, C.A.; Dwiyantri, R.S.M. Seasonal Monitoring of Chlorophyll-a with Landsat 8 Oli in the Madura Strait, Pasuruan, East Java, Indonesia. *Geography. Environ. Sustain.* **2021**, *14*, 22–29. [CrossRef]

44. Meng, H.; Zhang, J.; Zheng, Z. Retrieving Inland Reservoir Water Quality Parameters Using Landsat 8- 9 OLI and Sentinel-2 MSI Sensors with Empirical Multivariate Regression. *Int. J. Environ. Res. Public Health* **2022**, *19*, 7725. [[CrossRef](#)] [[PubMed](#)]
45. Buma, W.G.; Lee, S.-I. Evaluation of Sentinel-2 and Landsat 8 Images for Estimating Chlorophyll-a Concentrations in Lake Chad, Africa. *Remote Sens.* **2020**, *12*, 2437. [[CrossRef](#)]
46. Brenes, G.C.; Alpizar, L.H.; Perez, I.A. Chlorophyll-a Modeling in the Sierpe River with Sentinel-2 and Google Earth Engine. In Proceedings of the 2022 IEEE 4th International Conference on BioInspired Processing (BIP), Cartago, Costa Rica, 15–17 November 2022; pp. 1–5. [[CrossRef](#)]
47. Ha, N.T.T.; Thao, N.T.P.; Koike, K.; Nhuan, M.T. Selecting the Best Band Ratio to Estimate Chlorophyll-a Concentration in a Tropical Freshwater Lake Using Sentinel 2A Images from a Case Study of Lake Ba Be (Northern Vietnam). *ISPRS Int. J. Geo-Inf.* **2017**, *6*, 290. [[CrossRef](#)]
48. Moradi, M.; Keivan, K. Spatio-Temporal Variability of Red-Green Chlorophyll-a Index from MODIS Data—Case Study: Chabahar Bay, SE of Iran. *Cont. Shelf Res.* **2019**, *184*, 1–9. [[CrossRef](#)]
49. Poddar, S.; Chacko, N.; Swain, D. Estimation of Chlorophyll-a in Northern Coastal Bay of Bengal Using Landsat-8 OLI and Sentinel-2 MSI Sensors. *Front. Mar. Sci.* **2019**, *6*, 598. [[CrossRef](#)]
50. Messineo, V.; Mattei, D.; Melchiorre, S.; Salvatore, G.; Bogialli, S.; Salzano, R.; Mazza, R.; Capelli, G.; Bruno, M. Microcystin diversity in a *Planktothrix rubescens* population from Lake Albano (Central Italy). *Toxicon* **2006**, *48*, 160–174. [[CrossRef](#)] [[PubMed](#)]
51. Bruno, M.; Messineo, V. Extraction and Quantification of BMAA from Water Samples. In *Protocols for Cyanobacteria Sampling and Detection of Cyanotoxin*; Thajuddin, N., Sankara Narayanan, A., Dhanasekaran, D., Eds.; Springer: Singapore, 2023. [[CrossRef](#)]
52. Morel, A.; Maritorena, S. Bio-optical properties of oceanic waters: A reappraisal. *J. Geophys. Res.* **2001**, *106*, 7163–7180. [[CrossRef](#)]
53. Knapp, D.; Fernández Castro, B.; Marty, D.; Loher, E.; Köster, O.; Wüest, A.; Posch, T. The Red Harmful Plague in Times of Climate Change: Blooms of the Cyanobacterium *Planktothrix rubescens* Triggered by Stratification Dynamics and Irradiance. *Front. Microbiol.* **2021**, *25*, 705914. [[CrossRef](#)] [[PubMed](#)] [[PubMed Central](#)]
54. Neil, C.; Spyrakos, E.; Hunter, P.; Tyler, A. A global approach for chlorophyll-a retrieval across optically complex inland waters based on optical water types. *Remote Sens. Environ.* **2019**, *229*, 159–178. [[CrossRef](#)]
55. Uudeberg, K.; Ansko, I.; Põru, G.; Ansper, A.; Reinart, A. Using Optical Water Types to Monitor Changes in Optically Complex Inland and Coastal Water. *Remote Sens.* **2019**, *11*, 2297. [[CrossRef](#)]
56. Free, G.; Bresciani, M.; Pinardi, M.; Peters, S.; Laanen, M.; Padula, R.; Cingolani, A.; Charavgis, F.; Giardino, C. Shorter Blooms Expected with Longer Warm Periods under Climate Change: An Example from a Shallow Meso-Eutrophic Mediterranean Lake. *Hydrobiologia* **2022**, *849*, 3963–3978. [[CrossRef](#)]

**Disclaimer/Publisher’s Note:** The statements, opinions and data contained in all publications are solely those of the individual author(s) and contributor(s) and not of MDPI and/or the editor(s). MDPI and/or the editor(s) disclaim responsibility for any injury to people or property resulting from any ideas, methods, instructions or products referred to in the content.